Shelling and Sinking Graphs on the Sphere

Jeff Erickson
University of Illinois Urbana-Champaign, IL, USA

Christian Howard
University of Illinois Urbana-Champaign, IL, USA

Abstract

We describe a promising approach to efficiently morph spherical graphs, extending earlier approaches of Awartani and Henderson [*Trans. AMS* 1987] and Kobourov and Landis [*JGAA* 2006]. Specifically, we describe two methods to morph shortest-path triangulations of the sphere by moving their vertices along longitudes into the southern hemisphere; we call a triangulation *sinkable* if such a morph exists. Our first method generalizes a longitudinal shelling construction of Awartani and Henderson; a triangulation is sinkable if a specific orientation of its dual graph is acyclic. We describe a simple polynomial-time algorithm to find a longitudinally shellable rotation of a given spherical triangulation, if one exists; we also construct a spherical triangulation that has no longitudinally shellable rotation. Our second method is based on a linear-programming characterization of sinkability. By identifying its optimal basis, we show that this linear program can be solved in $O(n^{\omega/2})$ time, where ω is the matrix-multiplication exponent, assuming the underlying linear system is non-singular. Finally, we pose several conjectures and describe experimental results that support them.

2012 ACM Subject Classification Theory of computation → Computational geometry

Keywords and phrases morphing, planar graphs, spherical graph drawing, longitudinal shelling

Digital Object Identifier 10.4230/LIPIcs.SoCG.2025.47

Related Version *Full Version*: `https://arxiv.org/abs/2504.05098` [24]

Acknowledgements The authors thank Eli Kujawa for early helpful discussions and the anonymous reviewers for their helpful comments and suggestions.

1 Introduction

A *morph* between two planar straight-line graphs is a continuous deformation from one to the other, such that all edges in all intermediate graphs are interior-disjoint line segments. Planar graph morphing has many applications in graphics, animation, visualization, and geometric modeling, as well as connections to fundamental questions in low-dimensional topology.

There are two state-of-the-art approaches for morphing planar graphs. The first is the barycentric interpolation method of Floater, Gotsman, and Surazhsky [26, 29, 31, 56–58], which is based on an extension by Floater [27, 28] of Tutte's classical spring-embedding theorem [60]. These algorithms compute an implicit representation of a smooth morph, any intermediate stage of which can be constructed in $O(n^{\omega/2}) = O(n^{1.1864})$ time, where $\omega < 2.3728$ is the matrix-multiplication exponent. The second method combines an edge-collapsing strategy originally proposed by Cairns [11,12,35,59] with more recent algorithms for convex hierarchical graph drawing [13, 17, 36, 39, 40]. This method has led to several efficient algorithms for constructing explicit representations of piecewise-linear morphs [2, 25, 39, 40]. Algorithms are also known for several variants of planar morphing [5, 6, 10, 15, 43, 61].

Both planar morphing approaches have recently been generalized to geodesic graphs on the flat torus [14, 25, 44], and very recently, Luo, Wu, and Zhu generalized the barycentric interpolation method to arbitrary negative-curvature surfaces of higher genus [45, 46].

© Jeff Erickson and Christian Howard;
licensed under Creative Commons License CC-BY 4.0

1.1 What about the sphere?

In light of the long history of results for morphing planar graphs and their generalizations to higher-genus surfaces, it is surprising how little is known about morphing graphs on the sphere. Although embeddings on the sphere are *topologically* equivalent to embeddings in the plane, the different geometries of the two surfaces induce significantly different behavior.

In 1944, Cairns [12] proved that any two isomorphic shortest-path triangulations of the sphere are connected by a continuous family of shortest-path triangulations, using essentially the same edge-contraction strategy that he used for planar triangulations (but with more complex case analysis). A direct translation of Cairns's spherical morphing proof leads to an exponential-time algorithm; unlike his planar result, this is still the fastest algorithm known. In fact, as far as we are aware, this is the *only* algorithm known for morphing arbitrary spherical triangulations.

Morphing algorithms are known for a few special cases of spherical triangulations. Almost all of these algorithms operate by moving vertices along longitudes into the southern hemisphere, projecting the resulting "southern" triangulation into the plane, and applying a planar morphing algorithm. Awartani and Henderson [4] describe an algorithm to morph spherical triangulations that satisfy a certain **longitudinal shelling** condition using this strategy. They also prove that any triangulation with a *longitudinal seam*, meaning there is a longitude that does not cross the interior of any edge, satisfies their shelling condition. (We study Awartani and Henderson's shelling condition in more detail in Section 3.) Kobourov and Landis [41] describe an algorithm to morph between *Delaunay* triangulations via longitudinal morphs; their algorithm easily generalizes to **coherent** triangulations, which are central projections of arbitrary convex polyhedra. The same method is also implicit in Richter-Gebert's proof [47, Theorem 13.3.3] of classical theorems of Eberhard [21] and Steinitz [50] describing morphs between isomorphic convex polyhedra.

We call a sphere triangulation **sinkable** if it can be morphed along longitudes into the southern hemisphere. Every coherent triangulation is longitudinally shellable, and every longitudinally shellable triangulation is sinkable. Awartani and Henderson [4] describe an example of an unsinkable triangulation; it is not possible to move the vertices of their triangulation into the southern hemisphere without inverting at least one face. The simplest examples of unsinkable triangulation are the central projections of sufficiently twisted *Schönhardt polyhedra* [48], where the rotated faces are normal to the z-axis; see Figure 1.1. (Supnick proved that Schönhardt triangulations are the simplest non-coherent triangulations [54, 55]; our algorithm in Section 5 can be used to determine which of them are sinkable.)

The definitions of longitudinal shellability and sinkability depend on a specific choice of antipodal points as the north and south poles; neither property is invariant under rotations of the sphere. For example, a 90° rotation around the x-axis makes every Schönhardt triangulation in Figure 1.1 longitudinally shellable, and therefore sinkable.

1.2 Our Results

We describe a promising approach to efficiently morph shortest-path embeddings of graphs on the sphere, extending the previous results of Awartani and Henderson [4] and Kobourov and Landis [41]. At a high level, we propose finding suitable rotations of the sphere that allow the source and target embeddings to be pushed into the southern hemisphere along longitudes, thereby reducing to a planar morphing problem.

We emphasize that we do *not* develop this strategy into a complete algorithm; the existence of an efficient spherical morphing algorithm remains an open problem. We also note that sinking is not *required* to construct spherical morphs; for example, we can directly morph any Schönhardt triangulation into any other by twisting one face.

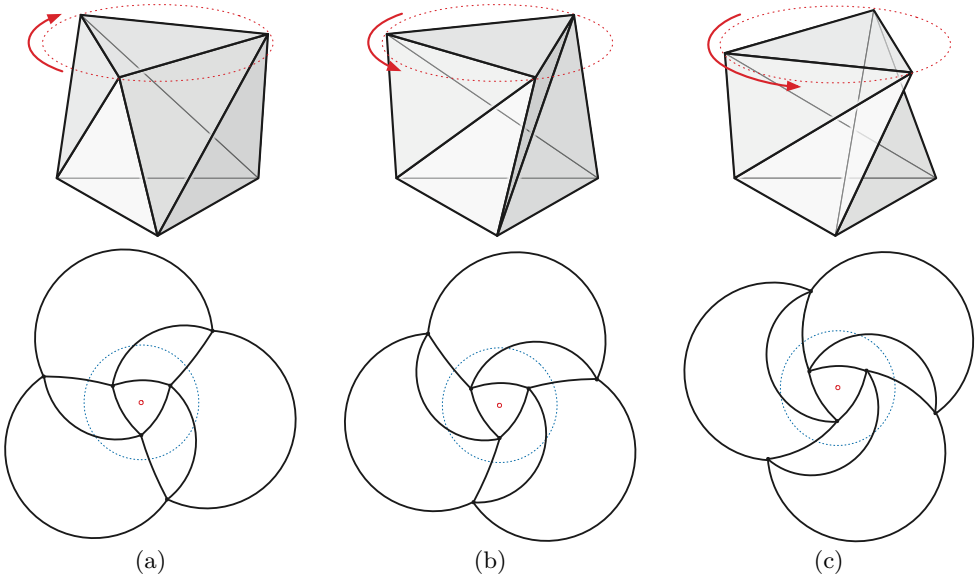

Figure 1.1 Three Schönhardt polyhedra and stereographic projections of the corresponding spherical triangulations. Depending on the twisting angle, these triangulations are (a) coherent and therefore longitudinally shellable, (b) sinkable but not longitudinally shellable, or (c) not sinkable.

We begin in Section 2 by reviewing relevant definitions, describing our proposed morphing strategy in detail, and proving some preliminary results. In Section 3, we formally define the *longitudinal shelling* condition introduced by Awartani and Henderson and provide several combinatorial characterizations, each of which can be tested in $O(n)$ time. We also reiterate Awartani and Henderson's proof that every longitudinally shellable triangulations is sinkable. In Section 4, we present an algorithm that either finds a rotation of a given sphere triangulation Γ that is longitudinally shellable, or reports correctly that no such rotation exists, in $O(n^{5/2}\log^3 n)$ time. We also construct a spherical triangulation that has no longitudinally shellable rotation. In Section 5, we describe an efficient algorithm to determine whether a given sphere triangulation is *sinkable*. First we show that sinkability is equivalent to the feasibility of a certain linear program with $O(n)$ variables and constraints. By identifying the optimal basis for this linear program, we show that it can be solved in $O(n^{\omega/2})$ time, assuming the underlying linear system is non-singular.

Due to space constraints, we defer several proofs and related results to the full version [24]. In particular, we describe the results of lightweight experiments, which suggest that "in practice" one can find a shellable rotation of a spherical triangulation by testing a small number of random rotations. We also present several open problems for further research, including several conjectures suggested by our experimental results.

2 Background and Preliminary Results

2.1 Cartography

We consider drawings of graphs on the unit sphere $S^2 = \{(x, y, z) \mid x^2 + y^2 + z^2 = 1\}$. The **north pole** is the point $(0, 0, 1)$; the **south pole** is the point $(0, 0, -1)$; the **equator** is the intersection of the unit sphere with the plane $z = 0$. A **longitude** is an open great-circular arc whose endpoints are the north and south poles. Every point except the poles lies on a unique longitude.

Throughout the paper, we fix an arbitrary simple maximal planar graph G with $n \geq 4$ vertices, arbitrarily indexed from 1 to n. An **embedding** of G on the sphere is an injective map from G to S^2, or less formally, a drawing of G where edges are arbitrary simple curves that intersect only at their shared endpoints. Every embedding of G on the sphere is a **triangulation**, meaning every face is bounded by a cycle of three distinct edges.

Unless explicitly indicated otherwise, we consider only **generic shortest-path** triangulations, meaning (1) every edge is a great-circular arc with length less than π; (2) no great circle contains more than two vertices, and (3) no great circle through the poles contains more than one vertex. Condition (1) is the natural spherical analogue of straight-line embeddings in the plane. Condition (3) implies that vertices lie on distinct longitudes.

Classical theorems of Steinitz [33, 49, 50] and Whitney [8, 62] imply that G has a unique embedding on the sphere, up to homeomorphism, which is a generic shortest-path triangulation. A **face of G** is a face of this essentially unique embedding. We sometimes identify each face as a triple (i, j, k) of vertices (or their indices) in counterclockwise order around its interior.

Every generic shortest-path triangulation has a unique **north face** whose interior contains the north pole and a unique **south face** whose interior contains the south pole. The remaining **non-polar** faces are of two types: An **up-face** has one vertex (called its **apex**) directly north of its opposite edge (called its **base**); symmetrically, a **down-face** has one vertex (its apex) directly south of its opposite edge (its base). The **legs** of a non-polar face f are the edges of f incident to the apex of f. The faces immediately north and south of any vertex i are respectively denoted $\boldsymbol{f_{\mathsf{above}}(i)}$ and $\boldsymbol{f_{\mathsf{below}}(i)}$. For each vertex i, $f_{\mathsf{above}}(i)$ is either the north face or a down-face, and $f_{\mathsf{below}}(i)$ is either the south face or an up-face. See Figure 2.1.

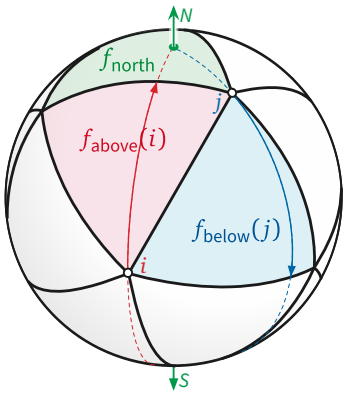

Figure 2.1 An up-face $f_{\mathsf{above}}(i)$, a down-face $f_{\mathsf{below}}(j)$, and the north face $f_{\mathsf{north}} = f_{\mathsf{above}}(j)$ of a spherical triangulation. Edge ij is a leg of both $f_{\mathsf{above}}(i)$ and $f_{\mathsf{below}}(j)$.

A face of a (generic) triangulation is **everted** if it has area greater than 2π, or equivalently, if it contains an open hemisphere. Every triangulation contains at most one everted face. We call a triangulation **full** if no face is everted, and **southern** if every vertex lies below the equator (which implies that the north face is everted).

A connected region R on the sphere is **θ-monotone** if every longitude is either disjoint from R or has connected intersection with R.

2.2 Coordinates

Throughout the paper, we represent spherical triangulations *implicitly* as projections of certain polyhedra onto the unit sphere. Specifically, we represent each vertex using signed homogeneous coordinates [51–53] – for any scalar $\lambda > 0$, the coordinate vectors (x, y, z) and $(\lambda x, \lambda y, \lambda z)$ represent the same point on the sphere. We can freely rescale the vertices, each independently, without changing the underlying spherical triangulation; although it is never actually necessary, this rescaling is sometimes convenient for purposes of discussion and intuition. For example, we can implicitly interpret any southern triangulation as a *planar* triangulation by scaling vertices onto the tangent plane $z = -1$; this scaling is equivalent to the *gnomonic* or *central* projection $(x, y, z) \mapsto (-x/z, -y/z, -1)$. Awartani and Henderson [4] analyze longitudinal morphing (defined below) by implicitly scaling vertices onto the unit cylinder $x^2 + y^2 = 1$.

2.3 Longitudinal Morphing

Two embeddings $\Gamma_0 \colon G \to S^2$ and $\Gamma_1 \colon G \to S^2$ are **isomorphic** if they define the same rotation system, or equivalently, if there is an orientation-preserving homeomorphism $H \colon S^2 \to S^2$ such that $\Gamma_1 = h \circ \Gamma_0$. Two isomorphic embeddings are **θ-equivalent** if each vertex of G lies on the same longitude in both embeddings.

A **homotopy** between two embeddings $\Gamma_0 \colon G \to S^2$ and $\Gamma_1 \colon G \to S^2$ is a continuous function $H \colon [0, 1] \times G \to S^2$ such that $H(0, \cdot) = \Gamma_0$ and $H(1, \cdot) = \Gamma_1$. Any pair of isomorphic embeddings Γ_0 and Γ_1 are connected by an **isotopy**, which is a homotopy H such that every intermediate drawing $\Gamma_t = H(t, \cdot)$ is an embedding. (The edges of these intermediate embeddings can be arbitrary simple curves, not necessarily shortest paths.) A **morph** is an isotopy in which the edges of every intermediate embedding Γ_t are shortest paths. Finally, a **longitudinal morph** is a morph in which vertices move only along their longitudes.

▶ **Lemma 2.1.** *Any two θ-equivalent triangulations are connected by a longitudinal morph.*

Proof sketch. Let Γ_0 and Γ_1 be two θ-equivalent triangulations. By scaling coordinate vectors as described in Section 2.2 if necessary, we can assume that each vertex has the same x- and y-coordinates in both embeddings. We define a longitudinal morph by linearly interpolating the z-coordinates of the vertices. The signed volume spanned by the vertices of any face is a linear function of the interpolation parameter t. Each non-polar face has the same orientation in Γ_0 and Γ_1, and therefore in every intermediate embedding. (See the full version [24] for a more detailed proof.) ◀

▶ **Corollary 2.2.** *A triangulation Γ is sinkable if and only if there is a southern triangulation that is θ-equivalent to Γ.*

We extend this argument slightly by considering **weak triangulations**, which are drawings of G that may include degenerate faces, but no inverted faces or crossing edges. (Weak triangulations are special cases of *weak embeddings* studied by Akitaya, Fulek, and Tóth [1] and Fulek and Kyncl [30].) A weak triangulation Γ_1 is θ-equivalent to a triangulation Γ_0 if vertices lie on the same longitudes in Γ_0 and Γ_1 and every non-degenerate non-polar face of Γ_i has the same orientation as the corresponding face of Γ_0.

▶ **Corollary 2.3.** *A triangulation Γ is sinkable if any only if there is a southern weak triangulation that is θ-equivalent to Γ.*

2.4 Morphing Strategy

Recall that a triangulation is **sinkable** if it can be longitudinally morphed to a θ-equivalent triangulation with all vertices below the equator. A **rotation** of a spherical triangulation Γ is the triangulation $\rho \circ \Gamma$ for some rigid motion $\rho\colon S^2 \to S^2$ of the sphere.[1] Our strategy rests on the following (admittedly optimistic) conjecture:

▶ **Conjecture 2.4.** *Every shortest-path triangulation Γ of the sphere can be rotated to obtain a sinkable triangulation.*

Conjecture 2.4 implies that one can morph any triangulation Γ_0 into any isotopic target triangulation Γ_1 through an intermediate coherent triangulation $\Gamma_{1/2}$. Steinitz's theorem [33, 49, 50] implies that a coherent embedding $\Gamma_{1/2}$ of G exists. Given any coherent triangulation, we can project its underlying convex polyhedron from a point on the positive z-axis just outside the polyhedron to the plane $z = -1$, and then centrally project the resulting planar triangulation back to the southern hemisphere, to obtain a θ-equivalent southern triangulation. It follows that *every* rotation of a coherent triangulation is sinkable.

We construct a morph from Γ_0 to $\Gamma_{1/2}$ in several stages as follows. First, we rotate Γ_0 so that the resulting triangulation Γ'_0 is sinkable (as guaranteed by Conjecture 2.4) and then longitudinally morph Γ'_0 to a southern triangulation Γ''_0.[2] Similarly, we rotate $\Gamma_{1/2}$ so that the resulting triangulation $\Gamma'_{1/2}$ has the same north face as Γ'_0 and Γ''_0, and then longitudinally morph $\Gamma'_{1/2}$ to a southern triangulation $\Gamma''_{1/2}$. Projection from the center of the sphere maps Γ''_0 and $\Gamma''_{1/2}$ to isomorphic straight-line triangulations in the plane $z = -1$, each with the same triangular outer face. We can construct a morph between these planar triangulations using any of several algorithms [2, 7, 11, 25, 29, 34, 40]; lifting this planar morph back to the sphere yields a spherical morph from Γ''_0 to $\Gamma''_{1/2}$. Our final morph is the concatenation of the rotation $\Gamma_0 \rightsquigarrow \Gamma'_0$, the longitudinal morph $\Gamma'_0 \rightsquigarrow \Gamma''_0$, the lifted planar morph $\Gamma''_0 \rightsquigarrow \Gamma''_{1/2}$, the reverse of the longitudinal morph $\Gamma'_{1/2} \rightsquigarrow \Gamma''_{1/2}$, and the reverse of the rotation $\Gamma_{1/2} \rightsquigarrow \Gamma'_{1/2}$. See Figure 2.2 for an example (without the initial and final rotations).

We construct a morph $\Gamma_1 \rightsquigarrow \Gamma_{1/2}$ using the same strategy. The final morph $\Gamma_0 \rightsquigarrow \Gamma_1$ is the concatenation of $\Gamma_0 \rightsquigarrow \Gamma_{1/2}$ and the reverse of $\Gamma_1 \rightsquigarrow \Gamma_{1/2}$.

3 Longitudinal Shelling

A **shelling** of a spherical triangulation Γ is an ordering $f_1, f_2, \ldots, f_{2n-4}$ of the faces of Γ such that the union of any prefix $U_k = \bigcup_{i \le k} f_i$ is either empty ($k = 0$), the entire sphere ($k = 2n - 4$), or a topological disk. We call a shelling **longitudinal** if every disk U_k is θ-monotone. Bruggesser and Mani's line shelling [9] implies that every *coherent* triangulation is longitudinally shellable.

3.1 Characterization

We characterize the shellability of Γ in terms of three directed graphs, which are illustrated in Figure 3.1.

[1] Rotations should not be confused with *rotation systems*, which encodes the cyclic order of edges around each vertex in a planar or spherical embedding.

[2] If the triangulation Γ_0 is not full, we can rotate it directly to a southern triangulation $\Gamma'_0 = \Gamma''_0$.

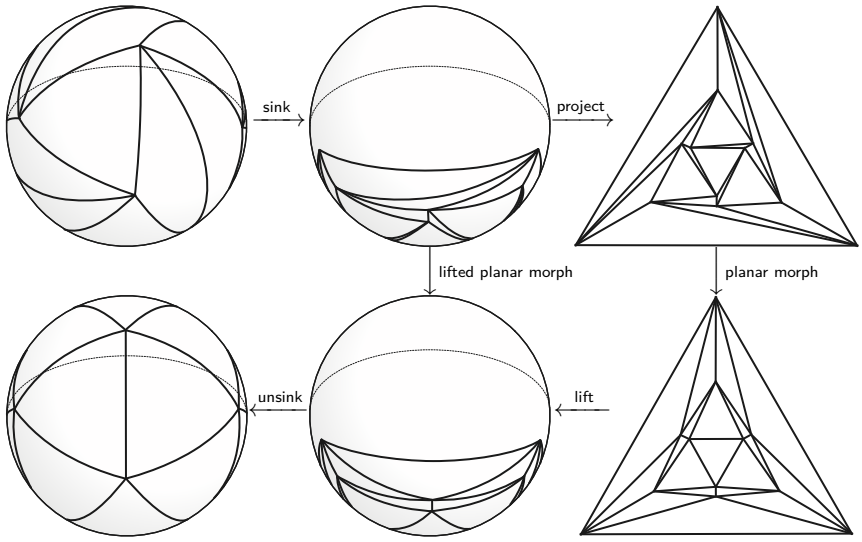

Figure 2.2 Morphing a six-beaked shaddock [19, 38] into a regular icosahedron; compare with Kobourov and Landis [41, Figure 1].

- The directed dual graph $\mathbf{\Gamma^{\downarrow}}$ contains a directed edge from face f_i to face f_j if and only if f_i and f_j share an edge in Γ, and some point in f_i is due north (on the same longitude) of some point in f_j.
- The oriented primal graph $\mathbf{\Gamma^{\rightarrow}}$ is the directed dual of $\Gamma^{\downarrow}$. For every undirected edge ij of Γ, the graph $\Gamma^{\rightarrow}$ contains the directed edge $i{\rightarrow}j$ if and only if vertex j is east of vertex i, or more formally, if the determinant

$$\det \begin{pmatrix} 0 & 0 & 1 \\ x_i & y_i & z_i \\ x_j & y_j & z_j \end{pmatrix} = \det \begin{pmatrix} x_i & y_i \\ x_j & y_j \end{pmatrix}$$

  is positive, where (x_i, y_i, z_i) is the coordinate vector for vertex i.
- Finally, $\mathbf{\Gamma^{\swarrow}}$ is a directed proper subgraph of Γ whose edges are the legs of each down-face, each directed toward its apex.

We defer the proof of the following lemma to the full version [24].

▶ **Lemma 3.1.** *For every generic shortest-path triangulation Γ, the following conditions are equivalent:*

(a) Γ *is longitudinally shellable.*
(b) $\Gamma^{\downarrow}$ *is acyclic.*
(c) $\Gamma^{\rightarrow}$ *is strongly connected.*
(d) $\Gamma^{\rightarrow}$ *contains directed paths from f_{north} to f_{south} and from f_{south} to f_{north}.*
(e) $\Gamma^{\swarrow}$ *is acyclic.*

Each of the conditions (b), (c), (d), and (e) can be tested in $O(n)$ time using textbook graph algorithms. A straightforward extension of Lemma 3.1 to triangulations with vertical edges implies a theorem of Awartani and Henderson [4]: Every triangulation with *longitudinal seam* is longitudinally shellable. See the full version [24] for more details.

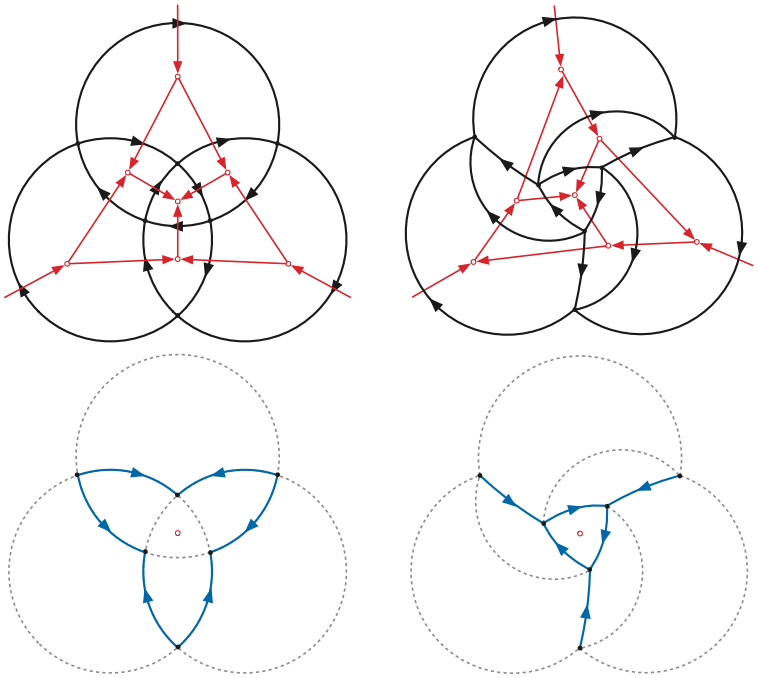

Figure 3.1 Stereographic projections of directed graphs $\Gamma^{\downarrow}$ (red straight edges), $\Gamma^{\rightarrow}$ (black curved edges), and $\Gamma^{\searrow\swarrow}$ (blue, second row) for the Platonic octahedral triangulation (which is longitudinally shellable) and a Schönhardt triangulation (which is not). Compare with Figure 1.1.

3.2 The Awartani–Henderson Embedding

▶ **Theorem 3.2** (Awartani and Henderson [4]). *Every longitudinally shellable triangulation of the sphere is sinkable. Moreover, given any longitudinally shellable triangulation Γ, we can compute a longitudinal morph from Γ to a southern triangulation in $O(n)$ time.*

Proof sketch. Let Γ be a longitudinally shellable triangulation. We construct a southern weak triangulation Γ' that is θ-equivalent to Γ by considering vertices in any topological order of $\Gamma^{\searrow\swarrow}$. The first three vertices lie on the north face and thus can be placed anywhere below the equator on their respective longitudes. For each later vertex i, we make z'_i as large as possible, such that no face induced by vertices 1 through i (except the north face) is inverted. Every down-face in the resulting drawing Γ' is degenerate. The theorem now follows from Corollary 2.3. (We give a more detailed proof, more closely following Awartani and Henderson [4], in the full version [24].) ◀

4 Longitudinally Shellable Rotations

When a given triangulation Γ is not longitudinally shellable, we can still apply our morphing strategy if we can find a rotation of the sphere that transforms Γ into a longitudinally shellable triangulation. In this section, we describe an efficient algorithm that either finds such a rotation or correctly reports that no such rotation exists. Our experimental results (described in the full version [24]) suggest that "in practice", even for triangulations with many long skinny triangles, a significant fraction of rotations of Γ are longitudinally shellable, so it suffices to consider a small number of random rotations. In fact, every one of the thousands of random adversarial triangulations we generated had shellable rotations. Nevertheless, in Section 4.2, we construct a triangulation with no longitudinally shellable rotation.

4.1 Finding a Shelling Direction

Instead of considering different rotations of Γ, it is convenient to keep Γ fixed and consider different locations for the "north pole". We call a unit vector p a **shelling direction** for Γ if any (and therefore every) rotation of the sphere that takes p to the standard north pole $(0, 0, 1)$ also takes Γ to a longitudinally shellable triangulation. We similarly define the directed graphs $\Gamma^{\downarrow}(p)$ and $\Gamma^{\rightarrow}(p)$ and $\Gamma^{\searrow\swarrow}(p)$. For example, for any unit vector $p = (x, y, z)$, the graph $\Gamma^{\rightarrow}(p)$ contains the edge $i{\rightarrow}j$ if and only if

$$\mathrm{vol}(p, i, j) := \det \begin{pmatrix} x & y & z \\ x_i & y_i & z_i \\ x_j & y_j & z_j \end{pmatrix} > 0,$$

and p is a shelling direction for Γ if and only if the graphs $\Gamma^{\downarrow}(p)$ and $\Gamma^{\searrow\swarrow}(p)$ are acyclic.

▶ **Theorem 4.1.** *Given any shortest-path triangulation Γ on the sphere, we can either compute a shelling direction for Γ or report correctly that no such direction exists, in $O(n^{2.5} \log^3 n)$ time.*

Proof. Each edge ij in Γ lies on a unique great circle; let $\mathcal{A}(\Gamma)$ denote the arrangement of all $3n - 6$ such great circles. For any two unit vectors p and q, the graphs $\Gamma^{\rightarrow}(p)$ and $\Gamma^{\rightarrow}(q)$ are identical if and only if p and q lie in the same cell of $\mathcal{A}(\Gamma)$. Thus, for any cell C, we can write $\Gamma^{\rightarrow}(C)$ to denote the graph $\Gamma^{\rightarrow}(p)$ for any $p \in C$. If C and C' are adjacent two-dimensional cells of $\mathcal{A}(\Gamma)$, then $\Gamma^{\rightarrow}(C)$ and $\Gamma^{\rightarrow}(C')$ differ in the direction of exactly one edge.

We can find a shelling direction for Γ in $O(n^3)$ time by constructing the great-circle arrangement $\mathcal{A}(\Gamma)$, and then for each two-dimensional cell C, check whether $\Gamma^{\rightarrow}(C)$ is strongly connected. (This arrangement is centrally symmetric, and the gnomonic projection of either hemisphere to any tangent plane is an arrangement of *lines*. Thus, we can use any classical algorithm to construct line arrangements [16, 22, 23].

We can speed up this naive algorithm using a data structure of Diks and Sankowski for reachability queries in dynamic directed plane graphs [18]. Diks and Sankowski's data structure maintains a directed planar graph with a fixed embedding, supports edge insertions and deletions that do not change the embedding in $O(\sqrt{n} \log^3 n)$ time, and supports queries of the form "Is there a directed path from vertex i to vertex j?" in $O(\sqrt{n} \log^2 n)$ time.

To use this data structure, we traverse the dual graph of the arrangement $\mathcal{A}(\Gamma)$. At each two-dimensional cell C, we perform two reachability queries in $\Gamma^{\rightarrow}(C)$ between the two polar faces. If both reachability queries succeed, then by Lemma 3.1(d), cell c contains a shelling direction. When we move from a cell C to a neighboring cell C', we delete one edge and insert its reversal. Altogether, we perform $O(n^2)$ queries and $O(n^2)$ updates. ◀

4.2 Unshellable From Every Direction

Regard each edge of the undirected dual graph Γ^* as a pair of opposing directed edges or **darts**. For any directed cycle γ^* of darts in Γ^*, the **polar region $P(\gamma^*)$** is the set of all north poles p such that the directed dual graph $\Gamma^{\downarrow}(p)$ contains every dart in γ^*. A unit vector p is a shelling direction for Γ if and only if $p \notin P(\gamma^*)$ for *every* directed dual cycle γ^*.

▶ **Lemma 4.2.** *For every directed cycle γ^* of darts in the dual graph Γ^*, the corresponding polar region $P(\gamma^*)$ is the interior of a convex spherical polygon, that is, the intersection of S^2 with a (possibly empty) open convex polyhedral cone.*

Proof. Let $i{\to}j$ be any dart in Γ, and let f and g be the faces incident to $i{\to}j$ on the left and right, respectively. The directed graph $\Gamma^{\downarrow}(p)$ contains the edge $f{\to}g$ if and only if $\mathrm{vol}(p,i,j) > 0$. The set of all points p satisfying this inequality is an open hemisphere $H(f{\to}g)$ bounded by the great circle through $i{\to}j$. Finally, the polar region $P(\gamma^*)$ of any dual cycle γ^* is the intersection of the hemispheres $H(f{\to}g)$ for all $f{\to}g \in \gamma^*$. ◀

A **rotor** is the subset of faces of Γ dual to any directed cycle γ^* in the dual graph Γ^*. We sketch the construction of a triangulation Γ containing a small number of rotors, whose polar regions cover the entire sphere. We describe our construction in terms of an arbitrary sufficiently small angular parameter $\varepsilon > 0$; in practice, it suffices to set $\varepsilon \approx 0.01 \approx 0.5°$.

First we define a simple *equatorial rotor*, which triangulates a belt of width $O(\varepsilon^2)$ around a great circle using $O(1/\varepsilon)$ isosceles triangles with aspect ratio $O(\varepsilon)$ and with all edges at angle $O(\varepsilon)$ from the great circle. The triangulation edges are consistently oriented so that for any north pole p sufficiently far from the rotor, the rotor defines a cycle in the directed dual graph $\Gamma^{\downarrow}(p)$. The polar region of (one orientation of) the rotor is a convex spherical polygon whose boundary has Hausdorff distance $O(\varepsilon)$ from the rotor itself. In particular, in the limit as ε approaches zero, this polar region approaches an open hemisphere.

Figure 4.1 Local structure of an equatorial rotor.

Our unshellable triangulation contains four modified equatorial rotors, whose central great circles are parallel to the faces of a regular tetrahedron. Let Q denote the arrangement of these four great circles; Q is the central projection of an inscribed semi-regular cuboctahedron; see Figure 4.2. Each pair of great circles meets at an angle of $\arccos(1/3) \approx 70.529°$.

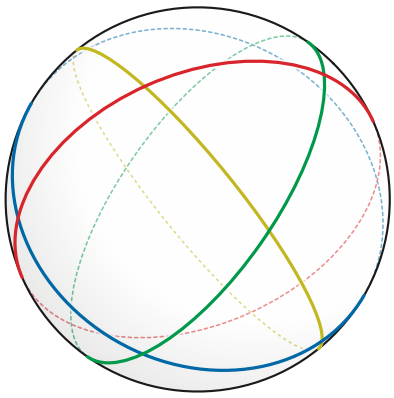

Figure 4.2 Four great circles defining a spherical cuboctahedron.

At each vertex of Q, we modify the two equatorial rotors by introducing a *crossing gadget*, illustrated in Figure 4.3(a). Overall the gadget resembles a rhombus with diameter $O(\varepsilon)$ whose edges are parallel to the great circles defining the rotors. Each of the equatorial rotors is broken and offset by $O(\varepsilon)$ to cover two opposite edges of this rhombus. Then three new edges are added to reconnect both rotors; these edges have distance and angle $O(\varepsilon)$ from the long diagonal of the rhombus and the bisector of the smaller angle between the two great circles. The two fat triangles inside the rhombus are incorporated into one of the two rotors (the vertical red rotor in Figure 4.3); the two thin triangles near the diagonal are incorporated into both. Figure 4.3(b) shows a schematic of our overall construction.

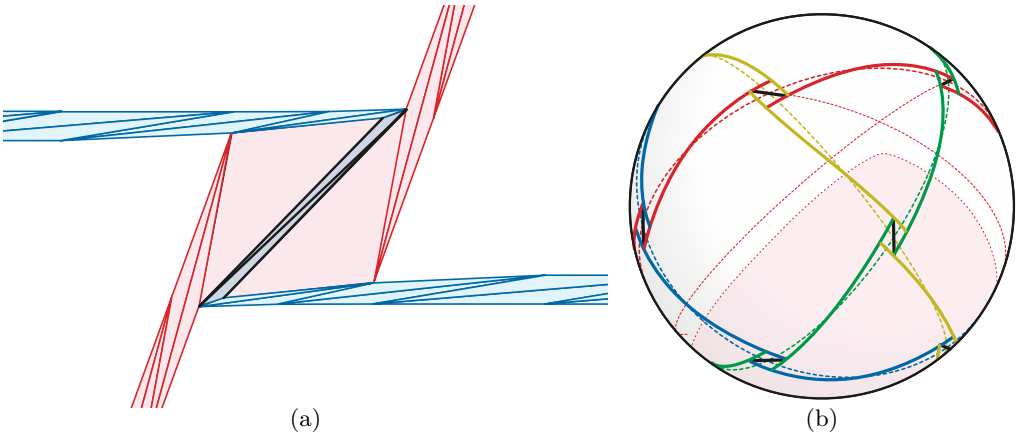

(a) (b)

Figure 4.3 (a) A single crossing gadget. (b) Constructing a triangulation with no shelling direction. Each color of broken lines is an equatorial rotor; each short black line is the diagonal of a crossing gadget. The polar region of one (red) equatorial rotor is shaded.

Now let γ^* be a directed cycle in the dual graph Γ^* through the faces of one equatorial rotor. The corresponding polar region $P(\gamma^*)$ nearly fills a triangular region bounded by three bisector circles, each defined by an antipodal pair of crossing gadgets. This polar region completely covers one triangular face and nearly half of three square faces of Q. The reversal of γ^* defines an antipodally symmetric polar region.

Thus, the union of the polar regions defined by all four equatorial rotors covers the entire sphere except for a small "hole" near the center of each square face of Q, which we can make arbitrarily small by choosing ε appropriately. We cover these holes by adding a small rotor, reminiscent of the projection of a Schönhardt polyhedron, inside each square face of Q; see Figure 4.4. Finally, to complete the triangulation Γ, we arbitrarily triangulate the area between the rotors.

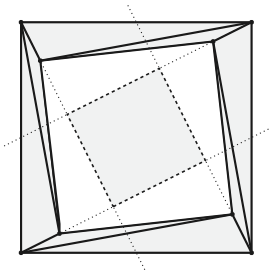

Figure 4.4 A square rotor (solid lines) and its polar region (dashed lines).

▶ **Theorem 4.3.** *There is a shortest-path triangulation of the sphere with no longitudinal shelling direction.*

Proof. By construction, every point $p \in S^2$ lies in the polar region of at least one rotor, and therefore in the polar region of at least one directed cycle in the dual graph Γ^*. Thus, for every $p \in S^2$, the directed dual graph $\Gamma^{\downarrow}(p)$ is not acyclic. The theorem follows immediately from Lemma 3.1. ◀

Nothing in our construction prevents our bad triangulation Γ from being *sinkable*. In particular, just before we add the final rotors to cover the "holes", the partial triangulation is still longitudinally shellable from any direction inside one of those holes. After rotating and sinking this partial triangulation and then projecting to the plane $z = -1$, we can add the final rotors to the resulting planar embedding. Moreover, experimental evidence [24] strongly suggests that every triangulation in which all edges have length less than $\pi/2$ is sinkable; our bad triangulation Γ satisfies this condition.

5 Sinking

Finally, we present an exact characterization of sinkable triangulations. Let Γ be our initial full shortest-path triangulation of the sphere. Recall from Corollary 2.3 that Γ is sinkable if and only if there is a southern weak triangulation Γ' that is θ-equivalent to Γ.

Without loss of generality we can consider only weak triangulations Γ' where each vertex has the same x- and y-coordinates as in Γ. Let (x_i, y_i, z_i) and (x_i, y_i, z'_i) denote the coordinates of vertex i in Γ and Γ', respectively. Then Γ' is θ-equivalent to Γ if and only if $\mathrm{vol}'(i,j,k) \geq 0$ for every non-polar face (i,j,k), where

$$\mathrm{vol}'(i,j,k) := \det \begin{pmatrix} x_i & y_i & z'_i \\ x_j & y_j & z'_j \\ x_k & y_k & z'_k \end{pmatrix}$$

We reiterate that because we have fixed all x- and y-coordinates, the volume determinant $\mathrm{vol}'(i,j,k)$ is a linear function of the vector z'.

▶ **Lemma 5.1.** *A spherical triangulation Γ is sinkable if and only if the following linear program is feasible:*

$$\begin{array}{lrll} \textit{maximize} & \sum_i z'_i & & \\ \textit{subject to} & z'_i = -1 & \textit{for every vertex } i \textit{ of } f_{\textit{north}} & (5.1) \\ & \mathrm{vol}'(i,j,k) \geq 0 & \textit{for every non-polar face } (i,j,k) & \end{array}$$

Proof. Suppose $z' = (z'_1, \ldots, z'_n)$ is the z-coordinate vector of a weak triangulation Γ' that is θ-equivalent to Γ, such that $z'_i < 0$ for all i. We can move the vertices of north face of Γ' to the plane $z = -1$ by applying a linear transformation that preserves the z-axis and all longitudes. The coordinate vector of every other vertex i is a positive linear combination of the north-face coordinate vectors, so $z'_i < 0$ for all i. ◀

Lemma 5.1 immediately implies an algorithm to compute a sinking longitudinal morph, or report correctly that none exists, in weakly polynomial time, provided the input x- and y-coordinates are rational [32]. We obtain a simpler and faster algorithm by identifying the optimal basis of the linear program, subject to a mild technical condition.

First we need a small extension of a result used in many planar morphing algorithms [17, 20, 37, 39, 40]. A polygon is *weakly convex* if its interior is convex and each of its vertices has interior angle *at most* π. Let T be any straight-line plane graph whose outer face is a simple x-monotone polygon and whose inner faces are triangles. A weakly convex polygon W is *compatible* with T if there is a homeomorphism from the boundary of T to the boundary of W that preserves x-coordinates. A weak planar triangulation T' is *x-equivalent* to T if it has the same underlying graph, every nondegenerate face of T' has the same orientation as the corresponding face of T, and corresponding vertices have equal x-coordinates.

▶ **Lemma 5.2.** *Given a triangulation T of an x-monotone polygon in the plane, and a weakly convex polygon W that is compatible with T, there is a weak planar triangulation T' that is x-equivalent to T and whose outer face is W.*

Proof sketch. If W is a *strictly* convex polygon (all interior angles are strictly less than π), the lemma follows immediately from algorithms of Chrobak, Goodrich, Tammassia [17] and Kleist, Klemz, Lubiw, Schlipf, Staals, and Strash [39]; we extend these algorithms to weakly convex W using a limiting argument. See the full version [24] for a complete proof. ◀

We emphasize that our algorithms never *compute* the weak triangulation T'; we only need to prove that it exists.

▶ **Theorem 5.3.** *If $z' = (z'_1, \ldots, z'_n)$ is an optimal solution to linear program* (5.1)*, then z' is also a solution to the following $n \times n$ linear system:*

$$\begin{aligned} z'_i &= -1 && \text{for every vertex } i \text{ of } f_{\mathsf{north}} \\ \mathrm{vol}'(i,j,k) &= 0 && \text{for every down-face } (i,j,k) \end{aligned} \tag{5.2}$$

Proof. Let z' be any feasible solution for linear program; Lemma 5.1 implies that $z'_i < 0$ for all i. Let Γ' be the southern weak triangulation defined by z', and suppose that at least one down-face of Γ' is nondegenerate. We argue that we can construct another southern weak triangulation Γ'' (that is, another feasible solution z'' to (5.1)) by increasing some z-coordinates and leaving all other coordinates fixed, which implies that z' is not an optimal solution to (5.1).

Call a vertex of Γ' *sober* if it is not incident to the north face or to any degenerate face. If any vertex of Γ' is sober, we can construct Γ'' by moving any sober vertex upward slightly and keeping all other vertices fixed. So without loss of generality, we assume that Γ' has no sober vertices. We call a vertex i *upward-free* if i is not a vertex of the north face and $f_{\mathsf{above}}(i)$ is nondegenerate in Γ', *downward-free* if $f_{\mathsf{below}}(i)$ is nondegenerate in Γ', *totally free* if it is both upward- and downward-free, and *trapped* if $f_{\mathsf{above}}(i)$ and $f_{\mathsf{below}}(i)$ are both degenerate.

A *bar* in Γ' is a maximal circular arc that is covered by edges of Γ' and has no totally free vertices in its interior. Each bar is either a single edge or the union of one or more degenerate faces; in the latter case, the corresponding subset of faces in Γ are edge-connected, and their union is a θ-monotone disk. Equivalently, a nontrivial bar is the image in Γ' of a maximal edge-connected subset of faces of Γ that are all degenerate in Γ'. We call the subcomplex of Γ induced by these faces a *pre-bar*. The *endpoints* of a pre-bar are the preimages of the endpoints of its bar. Because no vertex of Γ' is sober, every vertex not incident to the north face is contained in at least one bar.

Every upward-free vertex in Γ' is the image of a vertex on the northern boundary of a pre-bar in Γ. Every downward-free vertex in Γ' is either incident to the north face or the image of a vertex on the southern boundary of a pre-bar in Γ. Each endpoint of a bar can be upward-free, downward-free, or both. Finally, each trapped vertex in Γ' is the image of a vertex in the interior of a pre-bar in Γ, and thus lies on a unique bar in Γ'. See Figure 5.1(a) and (b).

We construct a new weak triangulation Γ'' by defining new coordinates $z''_i \geq z'_i$ for each vertex i. Let $\varepsilon > 0$ be any sufficiently small positive constant. Defining new coordinates for the free vertices of Γ' is straightforward:

- For every vertex i of the north face, we define $z''_i = z'_i$.
- For every upward-free vertex i, we define $z''_i = z'_i/(1+\varepsilon) > z'_i$.
- For every downward-free vertex i that is not also upward free, we define $z''_i = z'_i$.

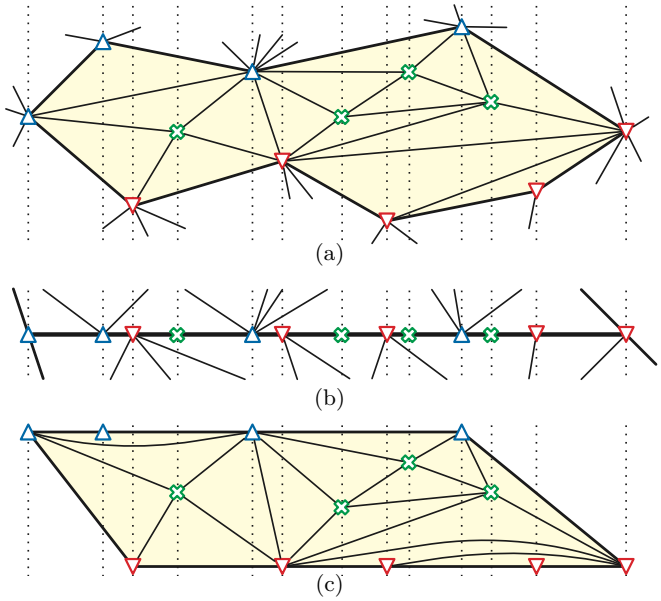

Figure 5.1 Planar projections of (a) a pre-bar in Γ, (b) the corresponding bar in Γ', and (c) the corresponding perturbed bar in Γ'' (with curved edges to show degenerate facets). Triangles indicate upward- and downward-free vertices; X's indicate trapped vertices. Dotted lines indicate longitudes.

Choosing sufficiently small ε already guarantees that any face that is non-degenerate in Γ' is also non-degenerate in Γ''. However, placing the trapped vertices to avoid inverting degenerate faces of Γ' requires more care.

Let β be any nontrivial bar in Γ', and let B be the corresponding pre-bar in Γ. We have already mapped the entire boundary of B to a spherical trapezoid τ in Γ''. Specifically, if β lies on the plane $z = ax + by$, then all upward-free vertices in β lie on the plane $z = (ax + by)/(1 + \varepsilon)$ in Γ''.

Because β projects to a line segment in the plane $z = -1$, it lies inside an open hemisphere bounded by a *vertical* plane through the origin. Without loss of generality, suppose β lies in the hemisphere $y > 0$. Let π_y denote the function $(x, y, z) \mapsto (x/y, z/y)$; we can interpret this function geometrically as the gnomonic projection from S^2 onto the plane $y = 1$. Then $\pi_y(\beta)$ is a non-vertical line segment, $\pi_y(B)$ is a triangulation of an x-monotone polygon, and $\pi_y(\tau)$ is a planar trapezoid whose lower boundary is a subset of $\pi_y(\beta)$ and whose upper boundary lies on a line parallel to $\pi_y(\beta)$. Each longitude ℓ through a trapped vertex i on β defines a *vertical* line $\pi_y(\ell)$ that must contain the point $(x_i/y_i, z_i''/y_i)$. See Figure 5.1.

To summarize, $\pi_y(B)$ is a triangulation of an x-monotone polygon, and $\pi_y(\tau)$ is a weakly convex polygon (specifically, a trapezoid) that is compatible with $\pi_y(B)$. Thus, Lemma 5.2 implies that there is a weak triangulation $\pi_y(T'')$ that is x-equivalent to $\pi_y(B)$ and whose outer face is $\pi_y(\tau)$. Pulling $\pi_y(T'')$ back to the sphere gives us a weak triangulation T'' of the spherical trapezoid τ that is θ-equivalent to B. Each interior vertex i of B maps to a vertex in the closed interior of τ, which implies $z_i' \le z_i'' \le z_i'/(1 + \varepsilon)$.

We assemble the overall weak triangulation Γ'' by applying this construction to every bar in Γ'. (Processing each bar requires projecting to a different vertical tangent plane.) Because $z_i'' \ge z_i'$ for every vertex i, and $z_i'' > z_i'$ for at least one vertex i, the original weak triangulation Γ' cannot be an optimal solution to our linear program (5.1). ◀

▶ **Corollary 5.4.** *Given a shortest-path triangulation* Γ *of the sphere, we can either compute a longitudinal morph from* Γ *to a southern triangulation, or report correctly that no such morph exists, in* $O(n^{\omega/2})$ *time, assuming linear system* (5.2) *is non-singular.*

Proof. The support of linear system (5.2) is precisely the directed planar graph $\Gamma^{\searrow\swarrow}$. Thus, assuming the system is non-singular, it can be solved in $O(n^{\omega/2}) = O(n^{1.1864})$ time (in the real RAM model) via nested dissection and fast matrix multiplication [3,42]. If the solution z' is a feasible point for linear program (5.1), the corresponding drawing Γ' is a weak southern triangulation θ-equivalent to Γ. If the system is non-singular, and the solution z' is not a feasible point for linear program (5.1), then by Theorem 5.3, the linear program is infeasible, so we can correctly report that Γ is not sinkable. ◀

Theorem 5.3 is a strict generalization of the Awartani-Henderson embedding, described in the proof of Theorem 3.2. When Γ is shellable, its support graph $\Gamma^{\searrow\swarrow}$ is acyclic. Thus, we can permute the rows and columns of (5.2) to obtain an upper-triangular system, which we can then solve by back-substitution. Each step of back-substitution assigns one z-coordinate, exactly mirroring one step of the Awartani-Henderson construction.

References

1. Hugo A. Akitaya, Radoslav Fulek, and Csaba D. Tóth. Recognizing weak embeddings of graphs. In *Proc. 29th Ann. ACM-SIAM Symp. Discrete Algorithms*, pages 274–292, 2018. doi:10.1137/1.9781611975031.20.
2. Soroush Alamdari, Patrizio Angelini, Fidel Barrera-Cruz, Timothy M. Chan, Giordano Da Lozzo, Giuseppe Di Battista, Fabrizio Frati, Penny Haxell, Anna Lubiw, Maurizio Patrignani, Vincenzo Roselli, Sahil Singla, and Bryan T. Wilkinson. How to morph planar graph drawings. *SIAM J. Comput.*, 46(2):824–852, 2017. doi:10.1137/16M1069171.
3. Noga Alon and Raphael Yuster. Matrix sparsification and nested dissection over arbitrary fields. *J. ACM*, 60(4):article 25, 18pp., 2013. doi:10.1145/2508028.2505989.
4. Marwan Awartani and David W. Henderson. Spaces of geodesic triangulations of the sphere. *Trans. Amer. Math. Soc.*, 304(2):721–732, 1987. doi:10.2307/2000738.
5. Fidel Barrera-Cruz, Penny Haxell, and Anna Lubiw. Morphing Schnyder drawings of planar triangulations. *Discrete Comput. Geom.*, 61(1):161–184, 2019. doi:10.1007/s00454-018-0018-9.
6. Therese Biedl, Anna Lubiw, and Jack Spalding-Jamieson. Morphing planar graph drawings via orthogonal box drawings. In *Proc. 32nd Int. Symp. Graph Drawing Network Vis.*, page to appear, 2024. doi:10.48550/arXiv.2409.04074.
7. R. H. Bing and Michael Starbird. Linear isotopies in E^2. *Trans. Amer. Math. Soc.*, 237:205–222, 1978. doi:10.2307/1997619.
8. Gunnar Brinkmann. A simple and elementary proof of Whitney's unique embedding theorem. *Ars Math. Contemp.*, 20(2):195–197, 2021. doi:10.26493/1855-3974.2334.331.
9. Heinz Bruggesser and Peter Mani. Shellable decompositions of cells and spheres. *Math. Scand.*, 29:197–205, 1971. doi:10.7146/math.scand.a-11045.
10. Kevin Buchin, William S. Evans, Fabrizio Frati, Irina Kostitsyna, Maarten Löffler, Tim Ophelders, and Alexander Wolff. Morphing planar graph drawings through 3D. In *Proc. 48th Int. Conf. Current Trends in Theory and Practice Comput. Sci. (SOFSEM)*, volume 13878 of *Lecture Notes Comput. Sci.*, pages 80–95. Springer, 2023. doi:10.1007/978-3-031-23101-8_6.
11. Stewart S. Cairns. Deformations of plane rectilinear complexes. *Amer. Math. Monthly*, 51(5):247–252, 1944. doi:10.2307/2304300.
12. Stewart S. Cairns. Isotopic deformations of geodesic complexes on the 2-sphere and on the plane. *Ann. Math.*, 45(2):207–217, 1944. doi:10.2307/1969263.

13 Jean Cerf. About the Bloch–Connelly–Henderson theorem on the simplexwise linear homeomorphisms of a convex 2-disk. Preprint, October 2019. doi:10.48550/arXiv.1910.00240.

14 Erin Wolf Chambers, Jeff Erickson, Patrick Lin, and Salman Parsa. How to morph graphs on the torus. In *Proc. 32nd Ann. ACM-SIAM Symp. Discrete Algorithms*, pages 2759–2778, 2021. doi:10.1137/1.9781611976465.164.

15 Steven Chaplick, Philipp Kindermann, Jonathan Klawitter, Ignaz Rutter, and Alexander Wolff. Morphing rectangular duals. In *Proc. 30th Int. Symp. Graph Drawing Network Vis.*, number 13764 in Lecture Notes Comput. Sci., pages 389–403. Springer, 2023. doi:10.1007/978-3-031-22203-0_28.

16 Bernard Chazelle, Leo J. Guibas, and D. T. Lee. The power of geometric duality. *BIT Numer. Math.*, 25(1):76–90, 1985. doi:10.1007/BF01934990.

17 Marek Chrobak, Michael T. Goodrich, and Roberto Tamassia. Convex drawings of graphs in two and three dimensions (preliminary version). In *Proc. 12th Ann. Symp. Comput. Geom.*, pages 319–328, 1996. doi:10.1145/237218.237401.

18 Krzysztof Diks and Piotr Sankowski. Dynamic plane transitive closure. In *Proc. 15th Ann. Europ. Symp. Algorithms*, number 4698 in Lecture Notes Comput. Sci., pages 594–604. Springer, 2007. doi:10.1007/978-3-540-75520-3_53.

19 Adrien Douady. Le shaddock à six becs. *Bull. APMEP*, 281:699–701, 1971. URL: https://www.apmep.fr/IMG/pdf/AAA71038.pdf.

20 Peter Eades, Qingwen Peng, Xuemin Lin, and Hiroshi Nagamochi. Straight-line drawing algorithms for hierarchical graphs and clustered graphs. *Algorithmica*, 44(1):1–32, 2006. doi:10.1007/s00453-004-1144-8.

21 Victor Eberhard. *Zur Morphologie der Polyeder*. Teubner, 1891.

22 Herbert Edelsbrunner and Leonidas J. Guibas. Topologically sweeping an arrangement. *J. Comput. Syst. Sci.*, 38(1):165–194, 1989. doi:10.1016/0022-0000(89)90038-X.

23 Herbert Edelsbrunner, Joseph O'Rourke, and Raimund Seidel. Constructing arrangements of lines and hyperplanes with applications. *SIAM J. Comput.*, 15(2):341–363, 1986. doi:10.1137/0215024.

24 Jeff Erickson and Christian Howard. Shelling and sinking graphs on the sphere. Preprint, April 2025. doi:10.48550/arXiv.2504.05098.

25 Jeff Erickson and Patrick Lin. Planar and toroidal morphs made easier. In *Proc. 29th Int. Symp. Graph Drawing Network Vis.*, number 12868 in Lecture Notes Comput. Sci., pages 123–137, 2021. doi:10.1007/978-3-030-92931-2_9.

26 Cesim Erten, Stephen G. Kobourov, and Chandan Pitta. Intersection-free morphing of planar graphs. In Giuseppe Liotta, editor, *Proc. 11th Symp. Graph Drawing*, volume 2912 of *Lecture Notes Comput. Sci.*, pages 320–331. Springer, 2003. doi:10.1007/978-3-540-24595-7_30.

27 Michael S. Floater. Parametrization and smooth approximation of surface triangulations. *Comp. Aided Geom. Design*, 14(3):231–250, 1997. doi:10.1016/S0167-8396(96)00031-3.

28 Michael S. Floater. Parametric tilings and scattered data approximation. *Int. J. Shape Modeling*, 4(3–4):165–182, 1998. doi:10.1142/S021865439800012X.

29 Michael S. Floater and Craig Gotsman. How to morph tilings injectively. *J. Comput. Appl. Math.*, 101(1–2):117–129, 1999. doi:10.1016/S0377-0427(98)00202-7.

30 Radoslav Fulek and Jan Kyncl. Hanani-Tutte for approximating maps of graphs. In *Proc. 34th Int. Symp. Comput. Geom.*, number 99 in Leibniz Int. Proc. Informatics, pages 39:1–39:15. Schloss Dagstuhl – Leibniz-Zentrum für Informatik, 2018. doi:10.4230/LIPIcs.SoCG.2018.39.

31 Craig Gotsman and Vitaly Surazhsky. Guaranteed intersection-free polygon morphing. *Computers & Graphics*, 25(1):67–75, 2001. doi:10.1016/S0097-8493(00)00108-4.

32 Martin Grötschel, László Lovász, and Alexander Schrijver. *Geometric Algorithms and Combinatorial Optimization*. Number 2 in Algorithms and Combinatorics. Springer-Verlag, 2nd edition, 1993. doi:10.1007/978-3-642-78240-4.

33 Branko Grünbaum. Graphs of polyhedra; polyhedra as graphs. *Discrete Math.*, 307(3–5):445–463, 2007. doi:10.1016/j.disc.2005.09.037.

34 Chung-Wu Ho. On certain homotopy properties of some spaces of linear and piecewise linear homeomorphisms. I. *Trans. Amer. Math. Soc.*, 181:213–233, 1973. doi:10.2307/1996630.

35 Chung-Wu Ho. Deforming P.L. homeomorphisms on a convex polygonal disk. *Pacific J. Math.*, 55(2):427–439, 1974. doi:10.2140/pjm.1974.55.427.

36 Seok-Hee Hong and Hiroshi Nagamochi. Convex drawings of hierarchical planar graphs and clustered planar graphs. *J. Discrete Algorithms*, 8(3):282–295, 2010. doi:10.1016/j.jda.2009.05.003.

37 John E. Hopcroft and Peter J. Kahn. A paradigm for robust geometric algorithms. *Algorithmica*, 7(1–6):339–380, 1992. doi:10.1007/BF01758769.

38 Børge Jessen. Orthogonal icosahedra. *Nordisk Matematisk Tidskrift*, 15(2/3):90–96, 1967. URL: https://www.jstor.org/stable/24524998.

39 Linda Kleist, Boris Klemz, Anna Lubiw, Lena Schlipf, Frank Staals, and Darren Strash. Convexity-increasing morphs of planar graphs. *Comput. Geom. Theory Appl.*, 84:69–88, 2019. doi:10.1016/j.comgeo.2019.07.007.

40 Boris Klemz. Convex drawings of hierarchical graphs in linear time, with applications to planar graph morphing. In *Proc. 29th Ann. Europ. Symp. Algorithms*, number 204 in Leibniz Int. Proc. Informatics, pages 57:1–57:15. Schloss Dagstuhl – Leibniz-Zentrum für Informatik, 2021. doi:10.4230/LIPIcs.ESA.2021.57.

41 Stephen G. Kobourov and Matthew Landis. Morphing planar graphs in spherical space. *J. Graph Algorithms Appl.*, 12(1):113–127, 2006. doi:10.7155/jgaa.00162.

42 Richard J. Lipton, Donald J. Rose, and Robert Endre Tarjan. Generalized nested dissection. *SIAM J. Numer. Anal.*, 16:346–358, 1979. doi:10.1137/0716027.

43 Anna Lubiw and Mark Petrick. Morphing planar graph drawings with bent edges. *J. Graph Algorithms Appl.*, 15(2):205–227, 2011. doi:10.7155/jgaa.00223.

44 Yanwen Luo, Tianqi Wu, and Xiaoping Zhu. The deformation space of geodesic triangulations of flat tori. Preprint, July 2021. doi:10.48550/arXiv.2107.05159.

45 Yanwen Luo, Tianqi Wu, and Xiaoping Zhu. The deformation space of geodesic triangulations and generalized Tutte's embedding theorem. *Geom. Topol.*, 7:3361–3385, 2023. doi:10.2140/gt.2023.27.3361.

46 Yanwen Luo, Tianqi Wu, and Xiaoping Zhu. Spaces of geodesic triangulations are cells. Preprint, August 2024. doi:10.48550/arXiv.2204.10833.

47 Jürgen Richter-Gebert. *Realization spaces of polytopes*. Number 1643 in Lecture Notes Math. Springer, 1996. doi:10.1007/BFb0093761.

48 Erich Schönhardt. Über die Zerlegung von Dreieckspolyedern in Tetraeder. *Math. Ann.*, 98(1):309–312, 1928. doi:10.1007/BF01451597.

49 Ernst Steinitz. Polyeder und Raumeinteilungen. *Enzyklopädie der mathematischen Wissenschaften mit Einschluss ihrer Anwendungen*, III.AB(12):1–139, 1916. URL: https://gdz.sub.uni-goettingen.de/id/PPN360609767.

50 Ernst Steinitz and Hans Rademacher. *Vorlesungen über die Theorie der Polyeder: unter Einschluß der Elemente der Topologie*. Number 41 in Grundlehren der mathematischen Wissenschaften. Springer-Verlag, 1934. Reprinted 1976. doi:10.1007/978-3-642-65609-5.

51 Jorge Stolfi. Oriented projective geometry. In *Proc. 3rd Ann. Symp. Comput. Geom.*, pages 76–85, 1987. doi:10.1145/41958.41966.

52 Jorge Stolfi. *Primitives for Computational Geometry*. Ph.D. thesis, Dept. Comput. Sci., Stanford, May 1988. Reprinted as Technical Report SRC-RR-36, DEC / HP Labs Systems Research Center, January 1989. URL: https://shiftleft.com/mirrors/www.hpl.hp.com/techreports/Compaq-DEC/SRC-RR-36.pdf.

53 Jorge Stolfi. *Oriented Projective Geometry: A Framework for Geometric Computations*. Academic Press, New York, NY, 1991. doi:10.1016/C2013-0-11551-6.

54 Fred Supnick. On the perspective deformation of polyhedra. *Ann. Math.*, 49(3):714–730, 1948. doi:10.2307/1969055.

55 Fred Supnick. On the perspective deformation of polyhedra. II. Solution of the convexity problem. *Math. Ann.*, 53(2):551–555, 1951. doi:10.2307/1969572.

56 Vitaly Surazhsky and Craig Gotsman. Controllable morphing of compatible planar triangulations. *ACM Trans. Graphics*, 20(4):203–231, 2001. doi:10.1145/502783.502784.

57 Vitaly Surazhsky and Craig Gotsman. Morphing stick figures using optimal compatible triangulations. In *Proc. 9th Pacific Conf. Comput. Graphics Appl.*, pages 40–49, 2001. doi:10.1109/PCCGA.2001.962856.

58 Vitaly Surazhsky and Craig Gotsman. Intrinsic morphing of compatible triangulations. *Int. J. Shape Modeling*, 9(2):191–201, 2003. doi:10.1142/S0218654303000115.

59 Carsten Thomassen. Deformations of plane graphs. *J. Comb. Theory Ser. B*, 34(3):244–257, 1983. doi:10.1016/0095-8956(83)90038-2.

60 William T. Tutte. How to draw a graph. *Proc. London Math. Soc.*, 13(3):743–768, 1963. doi:10.1112/plms/s3-13.1.743.

61 Arthur van Goethem and Kevin Verbeek. Optimal morphs of planar orthogonal drawings. In *Proc. 34th Int. Symp. Comput. Geom.*, number 99 in Leibniz Int. Proc. Informatics, pages 42:1–42:14. Schloss Dagstuhl – Leibniz-Zentrum für Informatik, 2018. doi:10.4230/LIPIcs.SoCG.2018.42.

62 Hassler Whitney. Congruent graphs and the connectivity of graphs. *Amer. J. Math.*, 54(1):150–168, 1932. doi:10.2307/2371086.